Research Square

Preprints are preliminary reports that have not undergone peer review.
They should not be considered conclusive, used to inform clinical practice,
or referenced by the media as validated information.

Dimethyl fumarate improves imiquimod-induced psoriasiform inflammation and melanogenesis

Ho Yong Hyun
Asan Medical Center
Joon Min Jung
Asan Medical Center
Jihun Choi
Asan Medical Center
Myoung Eun Choi
Asan Medical Center
Chong Hyun Won
Asan Medical Center
Youngsup Song
ysong@amc.seoul.kr

University of Ulsan
Sung Eun Chang
Asan Medical Center

Article

Keywords: Dimethyl Fumarate, Anti-melanogenic effects, Anti-inflammatory effects Keratinocytes

Posted Date: August 25th, 2026

DOI: https://doi.org/10.21203/rs.3.rs-10234125/v1

License: This work is licensed under a Creative Commons Attribution 4.0 International License.
Read Full License

Additional Declarations: No competing interests reported.

Abstract

Psoriasis is a chronic immune-mediated inflammatory disease characterized by IL-23/Th17 axis dysregulation. Dimethyl fumarate (DMF), an oral small-molecule fumaric acid ester as a NF-κB suppressor, is approved for the treatment of multiple sclerosis and psoriasis. Consistently, our clinical evaluation demonstrated that oral DMF administration led to significant clinical improvement in patients with plaque psoriasis. However, frequent gastrointestinal disturbances hindered its systemic administration, underscoring the necessity of investigating topical DMF. Therefore, we evaluated the efficacy of DMF administered either intraperitoneally or topically in a 4-day imiquimod-induced psoriasiform mouse model, finding that both routes comparably and significantly reduced clinical severity, inflammatory cell infiltration, and epidermal hyperplasia. Mechanistically, DMF suppressed the mRNA expression of TNF-α, IL-17C, and S100 families induced by M5 or IL-36γ stimulation in human keratinocytes. STAT3 phosphorylation as well as NF-κB p65 phosphorylation was well reduced. In contrast to most anti-psoriasis medications that aggravate hyperpigmentation, DMF reduced melanin content and tyrosinase activity in mouse melanocytes. Furthermore, DMF attenuated UVB-induced melanogenesis in an ex vivo human skin model, accompanied by the suppression of MITF and tyrosinase expression. In conclusion, DMF has another benefit of anti-melanogenic effects beyond anti-inflammatory effects. Topical DMF was also effective to reduce psoriatic inflammation as a promising alternative for psoriasis management.

Introduction

Psoriasis is a chronic immune-mediated inflammatory skin disorder characterized by well-demarcated, scaly erythematous papules or plaques. It commonly affects the scalp, elbows, knees, hands, feet, and trunk [1]. In addition to its typical clinical manifestations, inflammatory hyperpigmentation frequently occurs, particularly in patients with skin of color, even in the era of biologic therapies [2].

Psoriatic inflammation can be triggered in genetically predisposed individuals by various skin injuries [3]. Tissue damage leads to damage-associated molecular pattern (DAMP) release, which activates keratinocytes and dendritic cells [4–6]. Subsequent activation of Th17- and Th22-mediated immune responses establishes a self-amplifying inflammatory loop that sustains psoriatic lesions [7].

Keratinocytes constitute approximately 90% of epidermal cells and play a central role in both the initiation and amplification of psoriatic inflammation [8]. Keratinocyte hyperproliferation and abnormal differentiation are hallmarks of psoriatic lesions. Activated keratinocytes produce multiple immune mediators, including antimicrobial peptides, chemokines, cytokines, and S100 family alarmins, recruiting and activating immune cells within the skin [9, 10].

Although biologics have revolutionized psoriasis treatment, long-term disease management still requires safe and effective therapeutic options [11]. Topical treatments remain essential for patients with localized disease and for maintenance therapy. Therefore, researchers seek additional topical agents with anti-inflammatory efficacy and favorable safety profiles [12].

Dimethyl fumarate (DMF), a fumaric acid ester with immunomodulatory properties and antioxidant properties, has long been used as an oral therapeutic agent for multiple sclerosis and psoriasis [13–15]. Clinical studies and real-world evidence have demonstrated its efficacy and tolerability in psoriasis management [16, 17]. However, systemic DMF administration is frequently associated with adverse effects, including gastrointestinal disturbances such as diarrhea, nausea, and epigastric pain, as well as flushing and lymphopenia, which can limit patient compliance and long-term use.

DMF activates the nuclear factor erythroid 2-related factor 2 (NRF2) antioxidant response and modulates immune signaling pathways, inhibiting NF-κB activation [14, 18–20]. Through these mechanisms, DMF regulates both innate and adaptive immune responses and suppresses the production of pro-inflammatory cytokines involved in psoriatic inflammation [15, 21]. Notably, NF-κB inhibition has been associated with reduced melanogenesis in melanocytes [22]. Thus, DMF may possess dual therapeutic potential by attenuating both inflammatory pathways and pigmentation processes.

In this study, we investigated DMF's anti-inflammatory and anti-melanogenic effects and explored the underlying molecular mechanisms using in vitro, in vivo, and ex vivo models. Although clinical trials and real-world studies have consistently demonstrated systemic DMF's efficacy in moderate-to-severe plaque psoriasis, with significant improvements in PASI scores and quality of life [16, 23–29], its topical application remains underexplored. Therefore, we also evaluated topical DMF in an imiquimod-induced psoriasiform mouse model.

Results

DMF improved PASI and BSA in patients with plaque psoriasis

A total of 57 patients with plaque psoriasis were treated with oral DMF. Fourteen patients were excluded from analysis due to loss to follow-up or early discontinuation, leaving 43 patients available for the 16-week efficacy analysis. Mean PASI score decreased from 4.81 ± 3.89 at baseline to 3.06 ± 3.77 at week 16 (Fig. 1a, b) $p < 0.001$, with PASI50 and PASI75 achieved in 22 (51.2%) and 11 (25.6%) patients, respectively. BSA was similarly reduced from 4.35 ± 3.81% to 2.99 ± 3.07% (Fig. 1c) $p = 0.010$. Individual patient-level data are provided in **Supplementary Table 1.**

Systemic DMF administration suppresses IMQ-induced psoriasiform skin inflammation

Topical application of IMQ cream for four consecutive days induced progressive psoriasis-like skin inflammation characterized by pronounced erythema, scaling, and thickening (days 1–5). Conversely, systemic intraperitoneal (IP) administration of DMF during IMQ treatment markedly attenuated these lesions **(**Fig. 2a **and b)**.

Consistent with this, histological analysis showed that DMF treatment significantly alleviated IMQ-induced epidermal hyperplasia, resulting in reduced epidermal thickness (Fig. 2c). Immunohistochemical analysis further demonstrated that IP DMF markedly inhibited the IMQ-induced infiltration of $CD3^+$, $CD4^+$, $CD8^+$ T cells, along with $Ly6G^+$ neutrophils. Additionally, Ki-67-positive cellular proliferation was notably suppressed, as confirmed by quantification of DAB-positive areas (Fig. 2d). At the protein level, Western blot analysis revealed that systemic DMF treatment significantly reduced the expression of S100a7, S100a8, S100a9, Defb4, Tnf-α, and Il-17a (Fig. 2e). Similarly, qPCR analysis showed that *S100a8*, *S100a9*, *Tnf-α*, and *Il17c* mRNA levels were significantly decreased in IP DMF-treated mice compared with IMQ controls (Fig. 2f)

Topical DMF treatment suppresses IMQ-induced skin inflammation

Similar to the effects of systemic application, topical co-treatment with DMF one hour before IMQ application markedly alleviated psoriasiform inflammation (Fig. 3a and 3b). H&E staining demonstrated a significant increase in the IMQ group, which was markedly reversed by DMF treatment (Fig. 3c). Immunohistochemical analysis further revealed increased infiltration of $CD3^+$, $CD4^+$, and $CD8^+$ T cells, as well as $Ly6G^+$ neutrophils, alongside elevated Ki-67 expression in the IMQ group, all of which were markedely reduced in the DMF-treated group (Fig. 3d). Furthermore, Western blot analysis demonstrated that IMQ significantly upregulated the protein levels of S100a7, S100a8, S100a9, Defb4, Tnf-α, and Il-17a in dorsal skin tissues, all of which were significantly suppressed by DMF treatment (Fig. 3e). Consistent with these findings, *Tnfα*, *S100a8*, *S100a9*, *Il17c*, and *Il17f* mRNA levels were significantly increased in IMQ-treated skin and were markedly blunted by DMF (Fig. 3f).

DMF suppresses inflammatory and psoriasis-associated gene expression in keratinocytes stimulated with M5 or IL-36γ

DMF showed no significant cytotoxicity at the concentrations used (20 and 40 μM), as confirmed by an MTT assay (**Supplementary Fig. S1**). DMF inhibited LPS-induced p65 phosphorylation and iNOS expression, thereby reducing the production of inflammatory cytokines and nitric oxide in RAW 264.7 cells **(Supplementary Fig. S2)**. Similarly, DMF inhibited PMA-stimulated p65 phosphorylation, and the expression of its target inflammatory cytokines in Jurkat T cells **(Supplementary Fig. S3)** supporting its broad anti-inflammatory activity across multiple immune cell types.

To focus whether DMF influences keratinocyte inflammatory responses under different psoriatic conditions, we stimulated normal human keratinocytes (NHK) with an M5 cytokine cocktail or IL-36γ for six hours following a four-hour DMF pretreatment. M5 stimulation induced a robust upregulation of inflammatory cytokines, including *IL6, IL8, CCL20*, and *TNFα*, all of which were significantly suppressed by DMF pretreatment (Fig. 4a). Importantly, IL-36γ, a key cytokine implicated in generalized pustular psoriasis (GPP), also markedly increased *IL6, IL8, CCL20*, and *TNFα* expression, which was effectively attenuated by DMF (Fig. 4b). We next examined keratinocyte markers associated with psoriasis. M5

stimulation significantly increased the expression of *IL17C, IL36G, DEFB4, S100A7, S100A8*, and *S100A9*, all of which were downregulated by DMF pretreatment (Fig. 4c). Similarly, IL-36γ stimulation elevated the expression of *IL17C, IL36G, DEFB4*, and *S100* family members, and DMF also markedly inhibited their expressions (Fig. 4d).

DMF inhibits NF-κB and STAT3 signaling in M5- and IL-36γ–stimulated keratinocytes

To investigate the underlying mechanisms, we analyzed early signaling events using western blot analysis. M5 stimulation rapidly induced p65 and STAT3 phosphorylation as early as five minutes (Fig. 5a). However, DMF pretreatment markedly reduced the phosphorylation of both p65 and STAT3 without affecting total protein levels, indicating that DMF suppresses NF-κB and STAT3 signaling. At a later point (12 hours), M5 induced the upregulation of multiple S100 family proteins, which were substantially inhibited by DMF treatment (Fig. 5b).

IL-36γ stimulation triggered p65 phosphorylation at 10 minutes (Fig. 5c). IL-36γ–induced p65 phosphorylation was also attenuated by DMF pretreatment. Collectively, these results indicate that DMF attenuates keratinocyte inflammation by suppressing early NF-κB and STAT3 signaling, reducing downstream inflammatory mediator expression, by the inflammatory stimulators relevant to both plaque-type and pustular psoriasis.

DMF suppresses melanogenesis in murine melanocytes, human melanocytes, and ex vivo human skin

To investigate whether DMF modulates melanogenesis, we first assessed its effects in FSK-stimulated Mel-ab murine melanocytes. FSK treatment increased melanin content and tyrosinase activity, both of which were significantly inhibited by DMF treatment (Fig. 6a and 6b). Consistently, qRT-PCR and Western blot analyses demonstrated that DMF significantly reduced FSK-induced MITF and tyrosinase expression at both the mRNA **(**Fig. 6c**)** and protein **(**Fig. 6d**)** levels. We next evaluated the anti-melanogenic effects of DMF using a human *ex vivo* skin model with samples obtained from plastic surgery. UVB exposure markedly induced melanogenesis, as evidenced by an increase in melanin content measured by Fontana–Masson staining and the melanin index. DMF treatment significantly suppressed UVB-induced epidermal pigmentation **(**Fig. 6e**)**, which was accompanied by a potent reduction in UVB-induced MITF and tyrosinase mRNA expression at the transcriptional level **(**Fig. 6f**).**

Discussion

Psoriasis is driven by dysregulated crosstalk between keratinocytes and infiltrating immune cells, with the IL-23/Th17 axis playing a central pathogenic role [30]. Although biologics and Tyk2 inhibitor targeting this axis have markedly improved clinical outcomes, the need for safe and effective topical treatments and concerns for hyperpigmentation remain significant. In the present study, we investigated anti-inflammatory and anti-melanogenic effects of dimethyl fumarate (DMF). Using a well-established

imiquimod (IMQ)-induced psoriasiform mouse model, we also demonstrated that both topical and systemic DMF administration significantly reduced psoriasiform inflammation.

In our in vitro study using human keratinocytes, DMF directly suppressed inflammatory gene expression induced by both the M5 cytokine cocktail (IL-1α, TNF-α, IL-17A, IL-22 and oncostatin M) and IL-36γ stimulation. Notably, IL-36γ is a key cytokine in GPP, suggesting DMF's broader therapeutic relevance. Mechanistic analyses revealed that DMF inhibited NF-κB p65 phosphorylation and STAT3 phosphorylation in M5-stimulated NHKs. DMF also attenuated IL-36γ-induced p65 phosphorylation. DMF's dual inhibition of these pathways may explain its broad anti-inflammatory effects observed across multiple cell types and stimulatory conditions.

Uniquely, this study demonstrated DMF's anti-melanogenic properties. Hyperpigmentation is a very common and often distressing concern of psoriatic lesions, particularly in patients with skin of color [31–33]. DMF significantly reduced melanogenesis and UVB-induced melanin accumulation.

The demonstration that topical DMF achieves efficacy comparable to systemic administration in the IMQ model is particularly clinically significant. Indeed, Oral DMF has low patient compliance [19]. Topical formulations could potentially circumvent these systemic side effects while delivering therapeutic concentrations directly to affected skin. Although prior studies have reported dermal irritation and sensitization associated with topical DMF [34], we observed no significant skin irritation in the present study. Nevertheless, as NRF2 activation has been implicated in chemical-induced skin sensitization [35–38]. Thus strategies such as nanocarrier-based delivery systems [39, 40] or structural derivatives with attenuated NRF2-activating properties [41, 42] should be considered for topical application.

The present study has several limitations. The IMQ-induced murine model, while widely used, does not fully recapitulate the immunological and pathological complexity of human psoriasis. Future studies incorporating chronic treatment models and psoriatic patient-derived clinical specimens will be essential to clarify the broader therapeutic potential of DMF in psoriatic disease.

In summary, DMF suppressed keratinocyte-driven inflammatory responses in addition to the known anti-inflammatory effects in macrophages and T cells. It consistently downregulated S100 family proteins and DEFB4, which are known to perpetuate inflammatory feed-forward loops in psoriasis. Together with its anti-melanogenic effects, these findings support DMF's potential as both a systemic and topical therapeutic strategy for psoriasis and associated hyperpigmentation changes.

Materials and Methods

Cell lines and culture

Normal human keratinocytes (NHKs; KCLB, Seoul, South Korea) were cultured in EpiLife™ medium (Gibco, Waltham, MA, USA) supplemented with Human Keratinocyte Growth Supplement (HKGS; Invitrogen, Carlsbad, CA, USA) and 1% antibiotic–antimycotic (AA; Gibco). Raw 264.7 cells (KCLB) were

maintained in DMEM (Gibco) supplemented with 10% fetal bovine serum (FBS; Gibco) and 1% AA. Jurkat cells (ATCC, Manassas, VA, USA) were cultured in RPMI-1640 medium (Gibco) supplemented with 10% FBS and 1% AA. Mouse Melanocyte (Mel-Ab) cells [43, 44] were cultured in DMEM supplemented with 10% FBS and 1% AA, 100 nM TPA (Sigma-Aldrich, St. Louis, MO, USA), and 1 nM Cholera toxin (Sigma-Aldrich). All cells were maintained in a humidified incubator at 37°C with 5% CO_2.

Cell viability assay

Cell viability was assessed using the MTT assay (Sigma-Aldrich). Cells were seeded in 12-well plates and incubated for 24 h (Raw 264.7, Jurkat, and NHK) or 72 h (Mel-Ab) before MTT treatment. Formazan crystals were dissolved in DMSO, and absorbance was measured at 565 nm using a microplate reader (BioTek, Winooski, VT, USA).

Stimulation and treatment

Raw 264.7 cells were stimulated with lipopolysaccharide (LPS, 100 ng/mL) for four hours to measure mRNA expression by qRT-PCR, for one hour to evaluate protein expression by western blot, and finally for 24 hours to assess nitric oxide production. Jurkat T cells were stimulated with TPA (20 nM) for four hours for qPCR, then 15 minutes for western blot. Mel-ab cells were stimulated with forskolin (FSK; MedChemExpress, South Brunswick, NJ, USA) at 10 μM for 72 hours to evaluate melanin content, tyrosinase activity, mRNA expression by qPCR, and protein levels by western blot. To analyze gene expression via qPCR, NHK cells were treated for 6 hours with either a mixture of five cytokines (M5; 10 ng/mL each)—comprising IL-1α (BioLegend, San Diego, CA, USA), IL-17A (Biolegend), TNF-α (R&D Systems, Minneapolis, MN, USA), IL-22 (R&D Systems), and oncostatin M (BioLegend)—or with IL-36γ (Gibco; 200 ng/mL). For Western blot analysis of protein expression, cells were stimulated with M5 for 5 minutes or with IL-36γ for 10 minutes. .DMF was dissolved in DMSO to prepare a stock solution. Cells were pretreated with DMF (20 or 40 μM) for four hours before stimulation. The final DMSO concentration was kept constant in all groups, and vehicle controls received an equivalent amount of DMSO.

Nitric oxide assay

Nitric oxide (NO) production was measured in the culture supernatants of Raw 264.7 cells using the NO (Nitric Oxide) Plus Detection Kit (iNtRON Biotechnology, Seongnam, South Korea) according to the manufacturer's instructions. We measured absorbance at 540 nm using a microplate reader and calculated nitrite concentrations based on a sodium nitrite ($NaNO_2$) standard curve.

In vivo psoriasis model and DMF administration

8–10 weeks old female C57BL/6J mice (Jackson Lab, Bar Harbor, ME, USA) were used for all in vivo experiments. All animal procedures were performed in accordance with the protocols approved by the Institutional Animal Care and Use Committee of Asan Medical Center, Seoul, Korea (approval no. 2024-10-171). Psoriasiform inflammation was induced by daily topical application of 5% imiquimod (IMQ) cream (15 mg per mouse) to a 1 × 2 cm shaved area on the dorsal skin for four consecutive days. Before dorsal shaving and topical treatment, mice were anesthetized with 3% isoflurane for induction using a

small animal anesthesia system (Harvard Apparatus). For topical treatment, DMF (400 μM) was dissolved in an olive oil and acetone vehicle (1:4, v/v) and applied (100 μL per mouse) to the dorsal skin one hour before IMQ application each day. Control mice received the vehicle alone. For systemic treatment, DMF was administered via intraperitoneal injection at a dose of 50 mg/kg (100 μL per mouse) once daily, while control mice received the corresponding vehicle. Skin inflammation on the shaved dorsal back was evaluated daily using a modified PASI scoring system. Erythema, scaling, and skin thickness were each scored on a 0–4 scale (0, none; 1, slight; 2, moderate; 3, marked; 4, very marked), and the three scores were summed to give a cumulative clinical score ranging from 0 to 12. On day five, mice were euthanized by gradual CO_2 inhalation in a chamber according to the AAALAC guidelines, followed by the collection of dorsal skin tissues.

For RNA and protein analyses, the epidermis was separated from the dermis before extraction. Briefly, tissues were incubated at 56°C for 45 seconds and immediately transferred onto ice for 20 seconds, after which the epidermis was carefully peeled off. For histological and immunohistochemical analyses, whole skin tissues were fixed in 4% paraformaldehyde without separation.

Ex vivo human skin model

Human skin specimens were obtained from patients undergoing elective surgery after written informed consent. All procedures were approved by the Institutional Review Board of Asan Medical Center (IRB No. 2020-0091) and performed in accordance with the relevant guidelines and regulations. Immediately after excision, tissues were sequentially rinsed with 70–100% ethanol and maintained in phosphate-buffered saline (PBS) to prevent dehydration. The skin samples were trimmed into approximately 2 cm^2 pieces and placed in transwell inserts with the epidermal surface oriented upward to establish an air–liquid interface culture system. Explants were maintained at 37°C in a humidified incubator with 5% CO_2 and cultured in DMEM supplemented with 10% FBS and 10% AA. The culture medium was replaced daily. To induce melanogenesis, explants were irradiated with UVB at 200 mJ/cm^2 every 48 hours (two exposures in total), and tissues were harvested 96 hours after the first irradiation.

For treatment, we applied DMF to the epidermal surface in 30% propylene glycol and 70% ethanol. However, for medium treatment, we administered DMF in its DMSO-dissolved form. At the end of the experimental period, tissues were harvested. For qPCR analysis, the dermal layer was carefully removed using surgical scissors to isolate the epidermal tissue, and total RNA was extracted. For histological analysis, separate tissue samples were paraffin-embedded, sectioned, and melanin deposition was assessed by staining with a Fontana–Masson kit according to the manufacturer's instructions. The melanin index was quantified as the percentage of positively stained areas relative to the total tissue area using ImageJ software (NIH, Bethesda, MD, USA).

Clinical study

We retrospectively reviewed the medical records of patients with plaque psoriasis who were treated with oral dimethyl fumarate (DMF) at Asan Medical Center from December 2022 to February 2026 (IRB No. S2023-1914-0007). We initiated DMF at 120 mg/day and titrated up to a maximum of 720 mg/day. We

made dose adjustments or discontinuation decisions based on individual response and tolerability. PASI, BSA, and IGA were assessed at baseline and at week 16. We defined treatment response as a ≥ 50% (PASI50) or ≥ 75% (PASI75) reduction in PASI from baseline.

RNA extraction and quantitative PCR

We isolated total RNA from cultured cells using the Blood/Cultured Cell Total RNA Mini Kit (FABRK 001–2, Favorgen, Ping-Tung, Taiwan) according to the manufacturer's instructions. RNA concentration and purity were assessed using a NanoDrop spectrophotometer (Thermo Fisher Scientific, Waltham, MA, USA). Complementary DNA (cDNA) was synthesized using the RevertAid First Strand cDNA Synthesis Kit (K1622, Thermo Fisher Scientific) according to the manufacturer's instructions. Quantitative real-time PCR was performed using a SYBR Green Master Mix (Applied Biosystems, Foster City, CA, USA) on a LightCycler® 480 System (Roche, Basel, Switzerland) [45]. *GAPDH* was used as an internal control, and relative expression levels were calculated using the $2^{-\Delta\Delta Ct}$ method. Primer sequences are provided in **Supplementary Table 2**.

Western blot analysis

Protein extracts were prepared using 1% SDS lysis buffer, followed by the addition of 5× SDS sample buffer (Biosesang, Seoul, Korea). Samples were separated by SDS-polyacrylamide gel electrophoresis (SDS-PAGE) and transferred onto nitrocellulose membranes (Amersham, Marlborough, MA, USA). Membranes were blocked with 5% BSA in TBST for 1 hour at room temperature and then incubated overnight at 4°C with primary antibodies against p65 (ab16502, Abcam, Cambridge, UK), phospho-p65 (ab76302, Abcam), STAT3 (12640, Cell Signaling Technology, Danvers, MA, USA), phospho-STAT3 (9145, Cell Signaling Technology), S100A7 (A22271, ABclonal, Woburn, MA, USA), S100A8 (A12018, ABclonal), S100A9 (A9842, ABclonal), DEFB4 (A25636, ABclonal), TNF-α (ab6671, Abcam), IL-17A (ab79056, Abcam), MITF (ab12039, Abcam), tyrosinase (ab180753, Abcam), α-tubulin (AC012, ABclonal), and HSP90α/β (sc-13119, Santa Cruz Biotechnology, Santa Cruz, CA, USA). Protein bands were detected using an enhanced chemiluminescence (ECL) system (SuperSignal West Pico PLUS, 34580; SuperSignal West Femto, 34095, Thermo Fisher Scientific), and band intensities were quantified via densitometric analysis using ImageJ software. Protein levels were normalized to α-tubulin and HSP90α/β as loading controls

Immunohistochemistry (IHC) and H&E staining

Mouse back skin tissues were fixed in 4% paraformaldehyde, embedded in paraffin, and sectioned into slides. For immunohistochemical analysis, tissue sections underwent antigen retrieval using Antigen Unmasking Solution (H-3300-250, Vector Laboratories, Newark, CA, USA) according to the manufacturer's instructions. The sections were incubated with the following primary antibodies: CD3 (ab16669, Abcam), CD4 (ab183685, Abcam), CD8 (ab237723, Abcam), Ki-67 (ab16667, Abcam), and Ly6G (ab238132, Abcam). We performed immunostaining using the VECTASTAIN Elite ABC HRP Kit (Vector Laboratories, PK-6100), followed by visualization with 3,3'-diaminobenzidine (DAB). The sections were counterstained with hematoxylin. We performed hematoxylin and eosin (H&E) staining using

standard procedures. Images were captured using an Olympus SlideView VS200 system (Olympus, Tokyo, Japan). Positive staining was quantified as the percentage of DAB-positive areas using ImageJ software.

Melanin content and cellular tyrosinase activity assay

For melanin content measurement, cells were harvested in 1 N NaOH and incubated at 100°C for 30 minutes to solubilize melanin [33]. We measured absorbance at 405 nm using a microplate reader. Melanin content was normalized to the total protein concentration determined by Bradford protein assay (#5000006, Bio-Rad, Hercules, CA, USA) and expressed as a percentage of the control.

For cellular tyrosinase activity, cells were washed with ice-cold PBS and lysed in tyrosinase lysis buffer (phosphate buffer, pH 6.8, containing 1% Triton X-100) using repeated freeze–thaw cycles. We mixed 90 µL of the supernatant with 10 µL of 10 mM L-DOPA and incubated at 37°C. Tyrosinase activity was determined by measuring the absorbance at 475 nm every 10 minutes for at least one hour using a microplate reader and expressed as a percentage of the control.

Statistics

All data were expressed as the mean ± SEM; clinical data are presented as the mean ± SD. Statistical analysis was performed using GraphPad Prism (Version 8, San Diego, CA). *p*-values < 0.05, < 0.01, and < 0.001 were considered statistically significant (marked in the figures as *, **, and *** respectively).

Abbreviations

ultraviolet B radiation (UVB)

microphthalmia-associated transcription factor (MITF)

nuclear factor kappa B (NF-κB)

interleukin-1α (IL-1α)

interleukin-1β (IL-1β)

interleukin-6 (IL-6)

interleukin-8 (IL-8)

interleukin-17a (IL-17a)

interleukin-17c (IL-17c)

interleukin-17f (IL-17f)

interleukin-22 (IL-22)

defensin beta 4A (DEFB4A)

interleukin-36γ (IL-36γ)

tumor necrosis factor-α (TNF-α)

nitric oxide (NO)

glyceraldehyde-3-phosphate dehydrogenase (GAPDH)

C-C motif chemokine ligand 20 (CCL20)

reverse-transcription polymerase chain reaction (RT-PCR)

Normal Human Keratinocyte (NHK)

generalized pustular psoriasis (GPP)

intraperitoneally (IP)

Psoriasis Area and Severity Index (PASI)

Body Surface Area (BSA)

Investigator's Global Assessment (IGA)

12-o-tetradecanoylphorbol-13-acetate (TPA)

Declarations

Conflict of interest disclosures:

The authors have no conflict of interest to declare

Funding

This study was supported by grants from, Asan Institute for Life Sciences, Asan Medical Center, Seoul, Korea (2026IP0043-1), and the National Research Foundation of Korea (RS-2026-25468538)

Author Contribution

YS, CHW, and SEC conceptualized and supervised the study, and designed the experiments. HYH, JMJ, JC, and MEC developed the methodology. JMJ, JC, and MEC conducted the clinical study, HYH

performed the laboratory experiments, and HYH, JMJ, visualized the results, and curated the data. JMJ and SEC wrote the original draft. SEC and YS reviewed and edited the manuscript, and acquired the funding.

Acknowledgement

The authors would like to thank Dr. Hyun Ho Han of the Department of Plastic Surgery at Asan Medical Center for providing human skin samples.

Data Availability

All data generated or analyzed during this study are included in this published article and supplementary information files.

References

1. Griffiths, C. E. & Barker, J. N. Pathogenesis and clinical features of psoriasis. *Lancet* **370**, 263–271. 10.1016/S0140-6736(07)61128-3 (2007).
2. Alexis, A. F. & Blackcloud, P. Psoriasis in skin of color: epidemiology, genetics, clinical presentation, and treatment nuances. *J. Clin. Aesthet. Dermatol.* **7**, 16–24 (2014).
3. Kamiya, K., Kishimoto, M., Sugai, J., Komine, M. & Ohtsuki, M. Risk Factors for the Development of Psoriasis. *Int. J. Mol. Sci.* **20** 10.3390/ijms20184347 (2019).
4. Lande, R. et al. Plasmacytoid dendritic cells sense self-DNA coupled with antimicrobial peptide. *Nature* **449**, 564–569. 10.1038/nature06116 (2007).
5. Zhang, L. J. et al. Antimicrobial Peptide LL37 and MAVS Signaling Drive Interferon-beta Production by Epidermal Keratinocytes during Skin Injury. *Immunity* **45**, 119–130. 10.1016/j.immuni.2016.06.021 (2016).
6. Kim, D. H. & Jung, J. M. Pathophysiological roles of innate immune cells in psoriasis. *J. Korean Soc. Psoriasis*. **22**, 13–18. 10.23203/jksp.2025.22.1.13 (2025).
7. Res, P. C. et al. Overrepresentation of IL-17A and IL-22 producing CD8 T cells in lesional skin suggests their involvement in the pathogenesis of psoriasis. *PLoS One*. **5**, e14108. 10.1371/journal.pone.0014108 (2010).
8. Albanesi, C., Madonna, S., Gisondi, P. & Girolomoni, G. The Interplay Between Keratinocytes and Immune Cells in the Pathogenesis of Psoriasis. *Front. Immunol.* **9**, 1549. 10.3389/fimmu.2018.01549 (2018).
9. Cheng, J. B. et al. Transcriptional Programming of Normal and Inflamed Human Epidermis at Single-Cell Resolution. *Cell. Rep.* **25**, 871–883. 10.1016/j.celrep.2018.09.006 (2018).

10. Kim, J. et al. Single-cell transcriptomics applied to emigrating cells from psoriasis elucidate pathogenic versus regulatory immune cell subsets. *J. Allergy Clin. Immunol.* **148**, 1281–1292. 10.1016/j.jaci.2021.04.021 (2021).
11. Kamata, M. & Tada, Y. Efficacy and Safety of Biologics for Psoriasis and Psoriatic Arthritis and Their Impact on Comorbidities: A Literature Review. *Int. J. Mol. Sci.* **21** 10.3390/ijms21051690 (2020).
12. Segaert, S. et al. Long-term topical management of psoriasis: the road ahead. *J. Dermatolog Treat.* **33**, 111–120. 10.1080/09546634.2020.1729335 (2022).
13. Matteo, P. et al. New and Old Horizons for an Ancient Drug: Pharmacokinetics, Pharmacodynamics, and Clinical Perspectives of Dimethyl Fumarate. *Pharmaceutics* **14** 10.3390/pharmaceutics14122732 (2022).
14. Bresciani, G. et al. Novel potential pharmacological applications of dimethyl fumarate-an overview and update. *Front. Pharmacol.* **14**, 1264842. 10.3389/fphar.2023.1264842 (2023).
15. Bomprezzi, R. Dimethyl fumarate in the treatment of relapsing-remitting multiple sclerosis: an overview. *Ther. Adv. Neurol. Disord*. **8**, 20–30. 10.1177/1756285614564152 (2015).
16. Pellacani, G. et al. Efficacy and Safety of Dimethyl Fumarate in Patients with Moderate-to-Severe Plaque Psoriasis: DIMESKIN-2, a Multicentre Single-Arm Phase IIIb Study. *J. Clin. Med.* **11** 10.3390/jcm11164778 (2022).
17. Maul, L. V. et al. Dimethyl Fumarate Treatment for Psoriasis in Real-World Clinical Practice: An Analysis from the Swiss Registry. *Dermatology* **241**, 463–471. 10.1159/000548354 (2025).
18. Manai, F. & Amadio, M. Dimethyl Fumarate Triggers the Antioxidant Defense System in Human Retinal Endothelial Cells through Nrf2 Activation. *Antioxid. (Basel)*. **11** 10.3390/antiox11101924 (2022).
19. Bruck, J., Dringen, R., Amasuno, A., Pau-Charles, I. & Ghoreschi, K. A review of the mechanisms of action of dimethylfumarate in the treatment of psoriasis. *Exp. Dermatol.* **27**, 611–624. 10.1111/exd.13548 (2018).
20. Loewe, R. et al. Dimethylfumarate inhibits TNF-induced nuclear entry of NF-kappa B/p65 in human endothelial cells. *J. Immunol.* **168**, 4781–4787. 10.4049/jimmunol.168.9.4781 (2002).
21. McGuire, V. A. et al. Dimethyl fumarate blocks pro-inflammatory cytokine production via inhibition of TLR induced M1 and K63 ubiquitin chain formation. *Sci. Rep.* **6**, 31159. 10.1038/srep31159 (2016).
22. Moon, J. et al. Bay 11-7082, an NF-κB Inhibitor, Prevents Post-Inflammatory Hyperpigmentation Through Inhibition of Inflammation and Melanogenesis. *Pigment Cell. Melanoma Res.* **38**, e13207. 10.1111/pcmr.13207 (2025).
23. Mrowietz, U. et al. Efficacy and safety of LAS41008 (dimethyl fumarate) in adults with moderate-to-severe chronic plaque psoriasis: a randomized, double-blind, Fumaderm((R)) - and placebo-controlled trial (BRIDGE). *Br. J. Dermatol.* **176**, 615–623. 10.1111/bjd.14947 (2017).
24. Blair, H. A. & Dimethyl Fumarate A Review in Moderate to Severe Plaque Psoriasis. *Drugs* **78**, 123–130. 10.1007/s40265-017-0854-6 (2018).

25. Mrowietz, U. et al. Clinical use of dimethyl fumarate in moderate-to-severe plaque-type psoriasis: a European expert consensus. *J. Eur. Acad. Dermatol. Venereol.* **32** (Suppl 3), 3–14. 10.1111/jdv.15218 (2018).
26. van de Kerkhof, P. C. M. et al. Quality of life outcomes in adults with moderate-to-severe plaque psoriasis treated with dimethylfumarate (DMF): a post hoc analysis of the BRIDGE study. *J. Eur. Acad. Dermatol. Venereol.* **34**, 119–126. 10.1111/jdv.15922 (2020).
27. Corazza, M. et al. Dimethyl fumarate treatment for psoriasis in a real-life setting: A multicentric retrospective study. *Dermatol. Ther.* **34**, e15066. 10.1111/dth.15066 (2021).
28. Augustin, M. et al. Long-Term Treatment with Dimethyl Fumarate for Plaque Psoriasis in Routine Practice: Good Overall Effectiveness and Positive Effect on Impactful Areas. *Dermatol. Ther. (Heidelb)*. **12**, 1121–1131. 10.1007/s13555-022-00714-0 (2022).
29. Dauden, E. et al. Efficacy and Safety of Dimethyl Fumarate in Patients with Moderate-to-Severe Plaque Psoriasis: Results from a 52-Week Open-Label Phase IV Clinical Trial (DIMESKIN 1). *Dermatol. Ther. (Heidelb)*. **13**, 329–345. 10.1007/s13555-022-00863-2 (2023).
30. Lowes, M. A., Suarez-Farinas, M. & Krueger, J. G. Immunology of psoriasis. *Annu. Rev. Immunol.* **32**, 227–255. 10.1146/annurev-immunol-032713-120225 (2014).
31. Davis, E. C. & Callender, V. D. Postinflammatory hyperpigmentation: a review of the epidemiology, clinical features, and treatment options in skin of color. *J. Clin. Aesthet. Dermatol.* **3**, 20–31 (2010).
32. Amico, S. et al. Characteristics of postinflammatory hyper- and hypopigmentation in patients with psoriasis: A survey study. *J. Am. Acad. Dermatol.* **83**, 1188–1191. 10.1016/j.jaad.2020.02.025 (2020).
33. Lee, J. H., Yoo, J. M., Song, Y. & Chang, S. E. Hepatocyte growth factor suppresses melanogenesis via ERK-dependent nuclear exclusion of MITF. *Cell. Biosci.* 10.1186/s13578-026-01611-1 (2026).
34. de Haan, P., von Blomberg-van, B. M., de Groot, J., Nieboer, C. & Bruynzeel, D. P. The risk of sensibilization and contact urticaria upon topical application of fumaric acid derivatives. *Dermatology* **188**, 126–130. 10.1159/000247116 (1994).
35. El Ali, Z. et al. Allergic skin inflammation induced by chemical sensitizers is controlled by the transcription factor Nrf2. *Toxicol. Sci.* **134**, 39–48. 10.1093/toxsci/kft084 (2013).
36. Helou, D. G., Martin, S. F., Pallardy, M., Chollet-Martin, S. & Kerdine-Romer, S. Nrf2 Involvement in Chemical-Induced Skin Innate Immunity. *Front. Immunol.* **10**, 1004. 10.3389/fimmu.2019.01004 (2019).
37. Vallion, R. & Kerdine-Romer, S. Regulation of the immune response to contact sensitizers by Nrf2. *Contact Dermat.* **87**, 13–19. 10.1111/cod.14073 (2022).
38. Natsch, A. & Emter, R. Nrf2 activation as a key event triggered by skin sensitisers: The development of the stable KeratinoSens reporter gene assay. *Altern. Lab. Anim.* **44**, 443–451. 10.1177/026119291604400513 (2016).
39. Prow, T. W. et al. Nanoparticles and microparticles for skin drug delivery. *Adv. Drug Deliv Rev.* **63**, 470–491. 10.1016/j.addr.2011.01.012 (2011).

40. Natsch, A. & Emter, R. Skin sensitizers induce antioxidant response element dependent genes: application to the in vitro testing of the sensitization potential of chemicals. *Toxicol. Sci.* **102**, 110–119. 10.1093/toxsci/kfm259 (2008).
41. Bojanowski, K., Ibeji, C. U., Singh, P., Swindell, W. R. & Chaudhuri, R. K. A Sensitization-Free Dimethyl Fumarate Prodrug, Isosorbide Di-(Methyl Fumarate), Provides a Topical Treatment Candidate for Psoriasis. *JID Innov.* **1**, 100040. 10.1016/j.xjidi.2021.100040 (2021).
42. Hennig, P., Fenini, G., Di Filippo, M. & Beer, H. D. Electrophiles Against (Skin) Diseases: More Than Nrf2. *Biomolecules* 10, (2020). 10.3390/biom10020271
43. Kwon, H. et al. Semaxanib, a VEGF inhibitor, suppresses melanogenesis by modulating CRTC3 independently of VEGF signaling. *J. Dermatol. Sci.* **115**, 121–129. 10.1016/j.jdermsci.2024.07.004 (2024).
44. Lee, J. H. et al. Engineering small-molecule analogues of altiratinib via CREB-regulated transcription co-activator 3-target screening for the development of potent and safe topical therapeutics against skin hyperpigmentary diseases. *Clin. Transl Med.* **14**, e1625. 10.1002/ctm2.1625 (2024).
45. Yeo, H. et al. Diet-induced obesity and aging-induced upregulation of Trib3 interfere with energy homeostasis by downregulating the thermogenic capacity of BAT. *Exp. Mol. Med.* **56**, 2690–2702. 10.1038/s12276-024-01361-5 (2024).

Figures

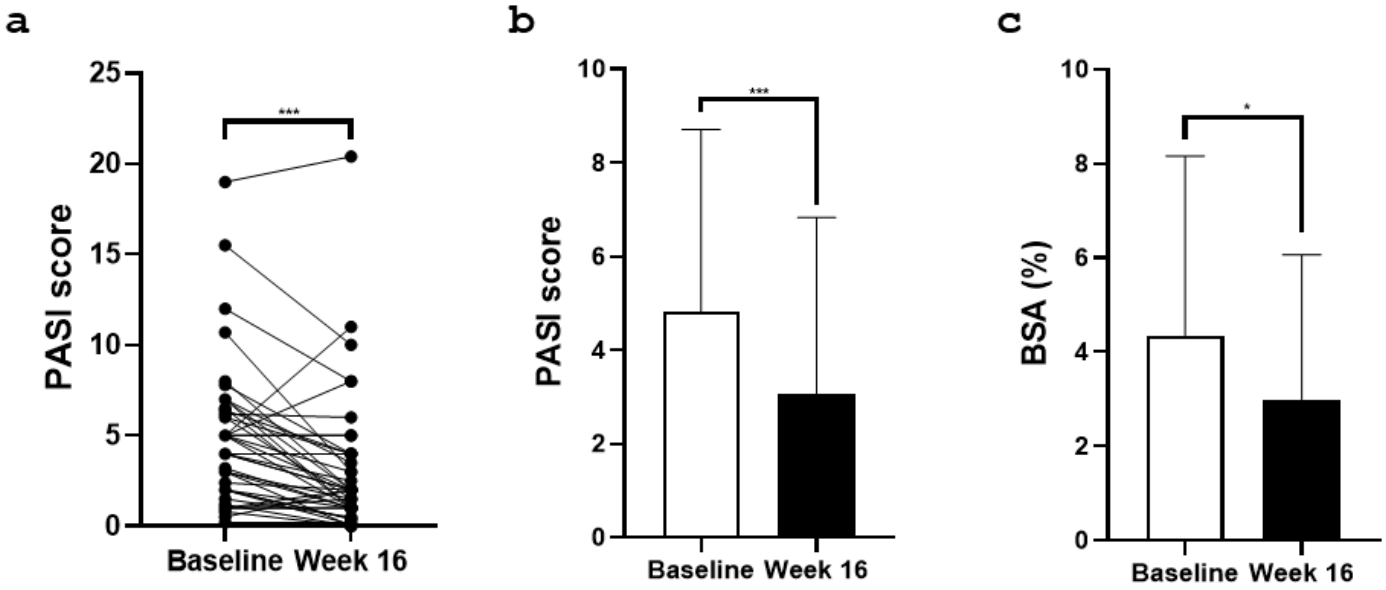


Figure 1

Oral DMF treatment significantly reduces PASI and BSA in patients with plaque psoriasis.

(a) Paired dot plot demonstrating individual PASI scores at baseline and week 16. Horizontal bars represent mean values. (b) Mean ± SD of PASI at baseline and week 16. (c) Mean ± SD of BSA (%) at baseline and week 16. Paired *t*-test. *$p < 0.05$, ***$p < 0.001$; $n = 43$.

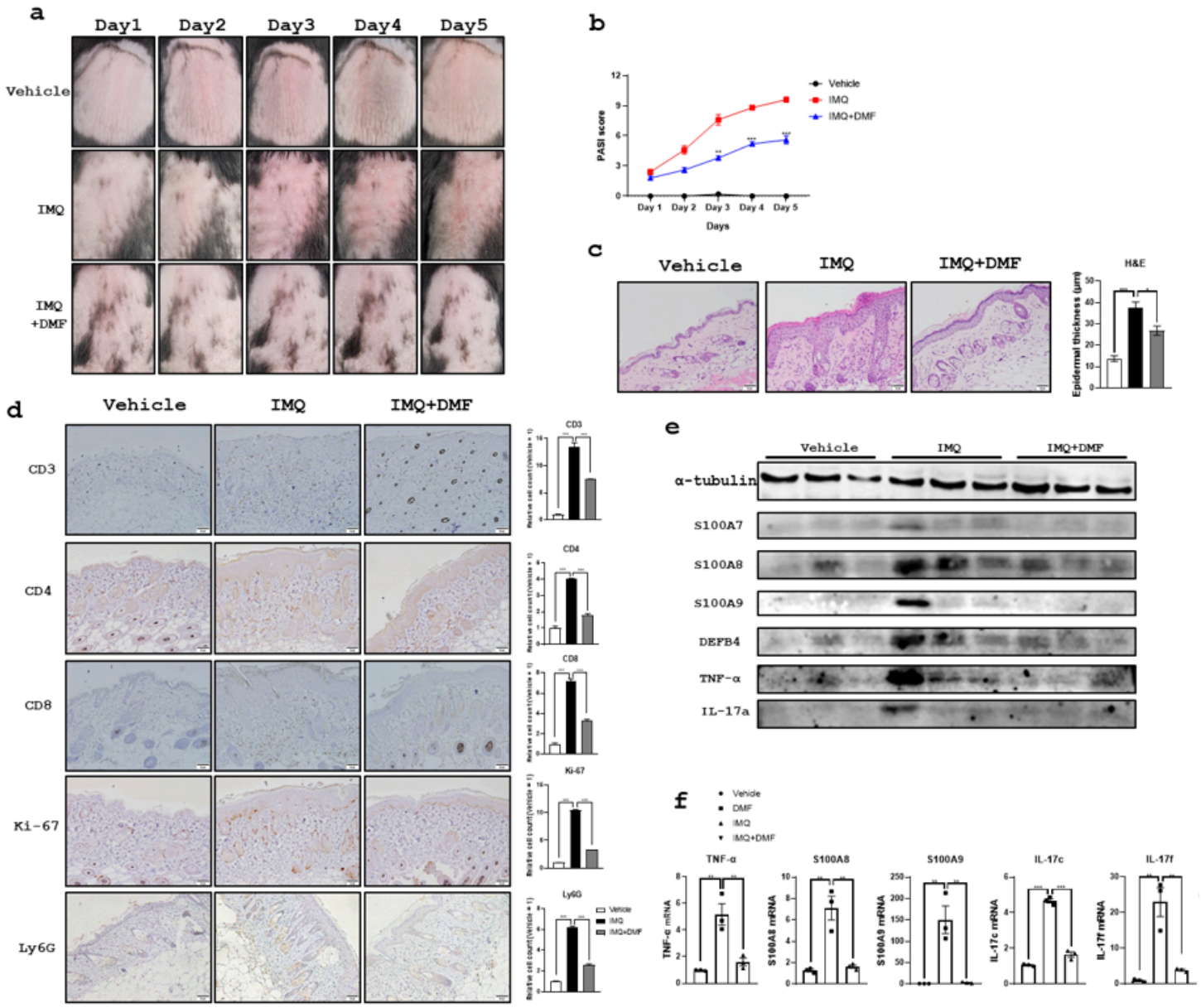


Figure 2

Intraperitoneal DMF administration attenuates IMQ-induced psoriasis-like skin inflammation.

(a) Representative dorsal skin images and (b) PASI scores of mice from Day 1 to Day 5 following topical IMQ application with or without intraperitoneal (IP) administration of DMF. (c) H&E staining of dorsal skin sections. Epidermal thickness was quantified at five randomly selected regions per section and expressed in μm. Scale bar = 50 μm. (d) Immunohistochemical staining for CD3, CD4, CD8, Ly6G, and Ki-67. DAB-positive areas were quantified using ImageJ threshold analysis and expressed as percentage of total area. Scale bar = 50 μm. (e) Western blot analysis of S100a7, S100a8, S100a9, Defb4, TNF-α, and IL-

17a protein expression with α-tubulin as a loading control. (f) qRT-PCR analysis of *TNF-α, S100a8, S100a9*, and *Il17c* mRNA expression normalized to *GAPDH*. Data are presented as mean ± SEM ($n \geq 5$ per group). Statistical significance was determined by one-way ANOVA followed by Tukey's multiple comparison test. *$p < 0.05$, **$p < 0.01$, ***$p < 0.001$.

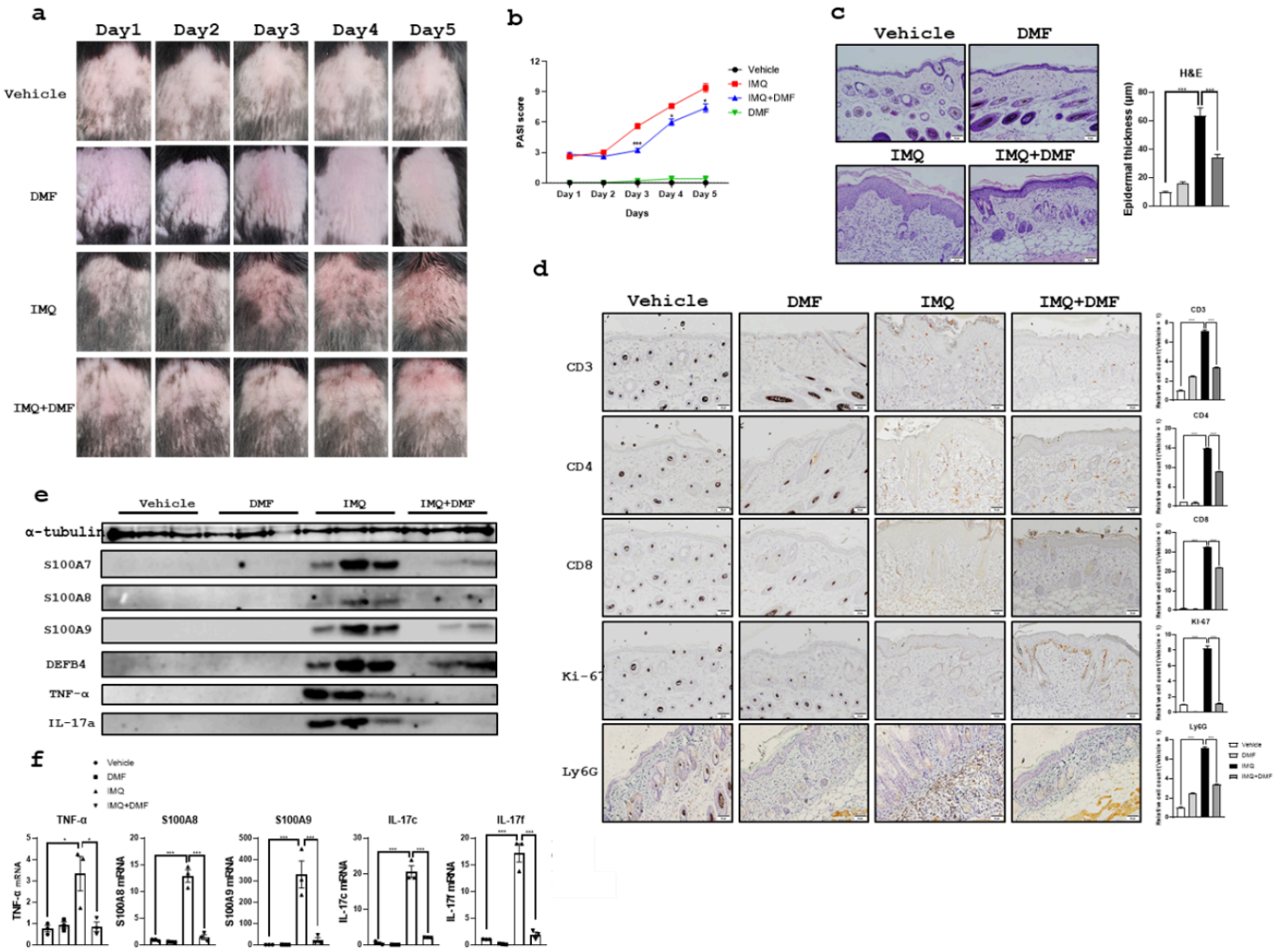


Figure 3

Topical DMF ameliorates IMQ-induced psoriasis-like skin inflammation.

(a) Representative dorsal skin images and (b) PASI scores of mice from Day 1 to Day 5 following topical IMQ application with or without topical DMF treatment. DMF was applied one hour prior to IMQ each day. (c) H&E staining of dorsal skin sections. Epidermal thickness was measured at five randomly selected sites per section and expressed in μm. Scale bar = 50 μm. (d) Immunohistochemical staining for CD3, CD4, CD8, Ly6G, and Ki-67. DAB-positive areas were quantified using ImageJ threshold analysis and expressed as percentage of total area. Scale bar = 50 μm. (e) Western blot analysis of S100a7, S100a8, S100a9, Defb4, TNF-α, and IL-17a protein expression with α-tubulin as a loading control. (f) qRT-PCR

analysis of *TNF-α, S100a8, S100a9*, and *Il17c* mRNA expression normalized to *GAPDH*. Data are presented as mean ± SEM ($n \geq 5$ per group). Statistical analysis was performed using one-way ANOVA followed by Tukey's multiple comparison test. *$p < 0.05$, **$p < 0.01$, ***$p < 0.001$.

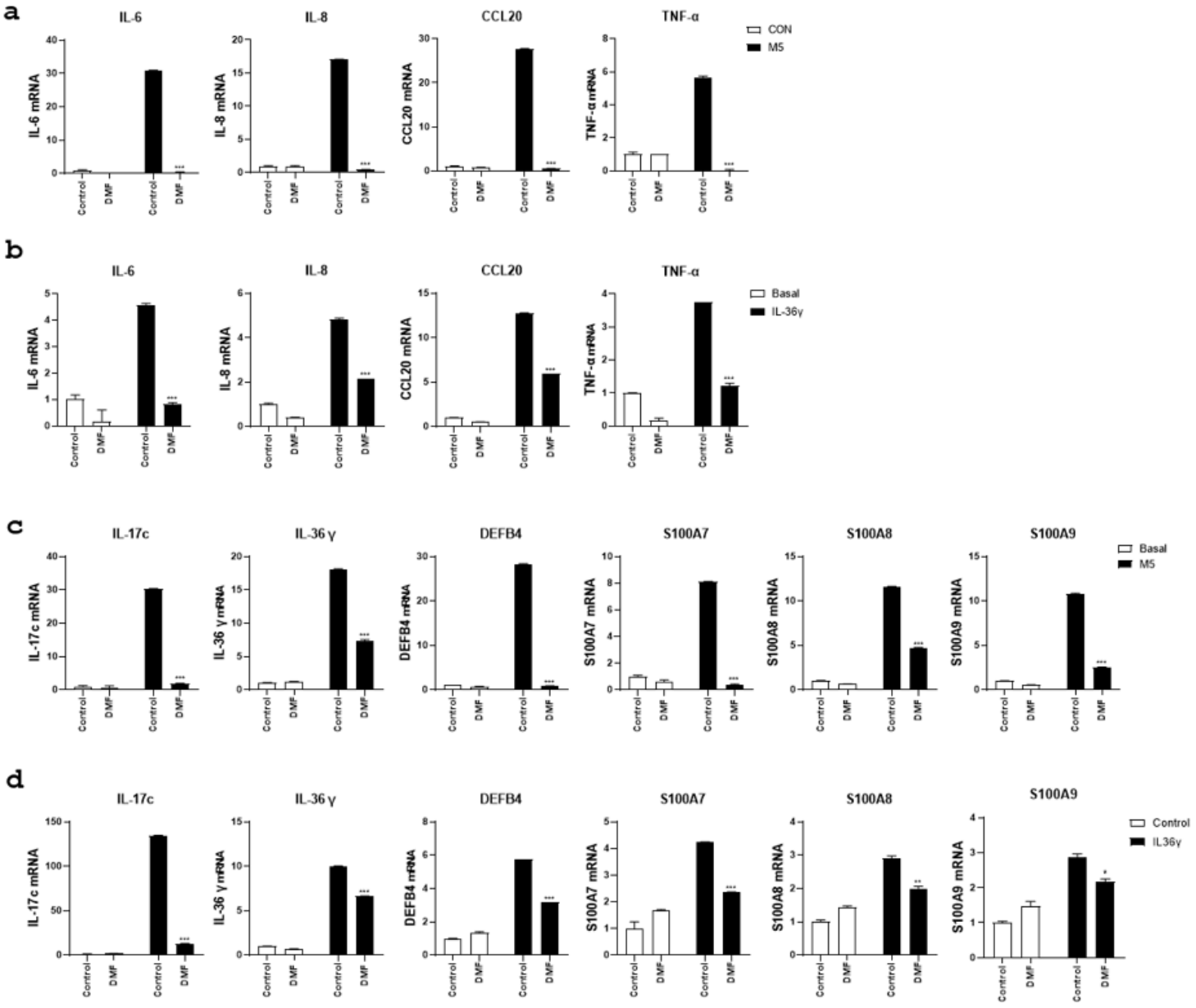


Figure 4

DMF suppresses M5- and IL-36γ–induced inflammatory and psoriasis-associated gene expression in NHKs.

Normal human keratinocytes (NHKs) were pretreated with DMF for four hours followed by stimulation with M5 cytokine cocktail or IL-36γ for six hours. (a) qRT-PCR analysis of M5-induced inflammatory cytokine mRNA levels (*IL6, IL8, CCL20, TNFA*). (b) qRT-PCR analysis of IL-36γ–induced inflammatory

cytokine mRNA levels (*IL6*, *IL8*, *CCL20*, *TNFA*). (c) qRT-PCR analysis of M5-induced psoriasis-associated keratinocyte marker mRNA levels (*IL17C*, *IL36G*, *DEFB4*, *S100A7*, *S100A8*, and *S100A9*). (d) qRT-PCR analysis of IL-36γ–induced psoriasis-associated keratinocyte marker mRNA levels (*IL17C*, *IL36G*, *DEFB4*, *S100A7*, *S100A8*, and *S100A9*). Gene expression levels were normalized to GAPDH. Data are presented as mean ± SEM from at least three independent experiments. Statistical analysis was performed using one-way ANOVA followed by Tukey's multiple comparison test. *$p < 0.05$, **$p < 0.01$, ***$p < 0.001$.

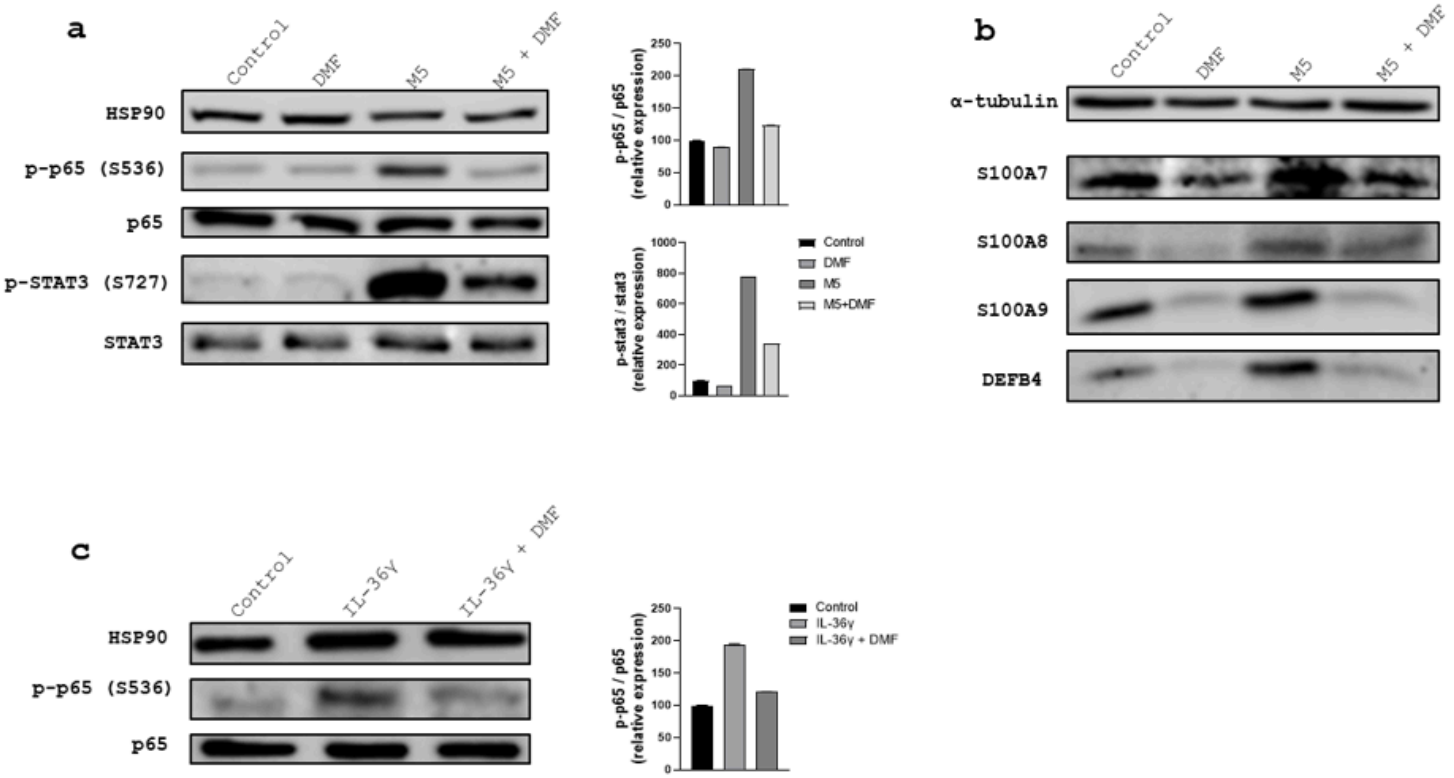


Figure 5

DMF inhibits NF-κB and STAT3 signaling in M5- and IL-36γ–stimulated NHKs.

We pretreated NHKs with DMF for four hours and stimulated with M5 or IL-36γ for the indicated time points. (a) Western blot analysis of phosphorylated (p-p65 and p-STAT3) and total p65 and STAT3 following five minutes of M5 stimulation. (b) Western blot analysis of S100 family and DEFB4 proteins expression following M5 stimulation (12 hours). (c) Western blot analysis of phosphorylated and total p65 following 10 minutes of IL-36γ stimulation. Representative blots from at least three independent experiments are given. Densitometric analysis was normalized to total protein levels and expressed as mean ± SEM. Statistical significance was determined using one-way ANOVA followed by Tukey's multiple comparison test. *$p < 0.05$, **$p < 0.01$, ***$p < 0.001$.

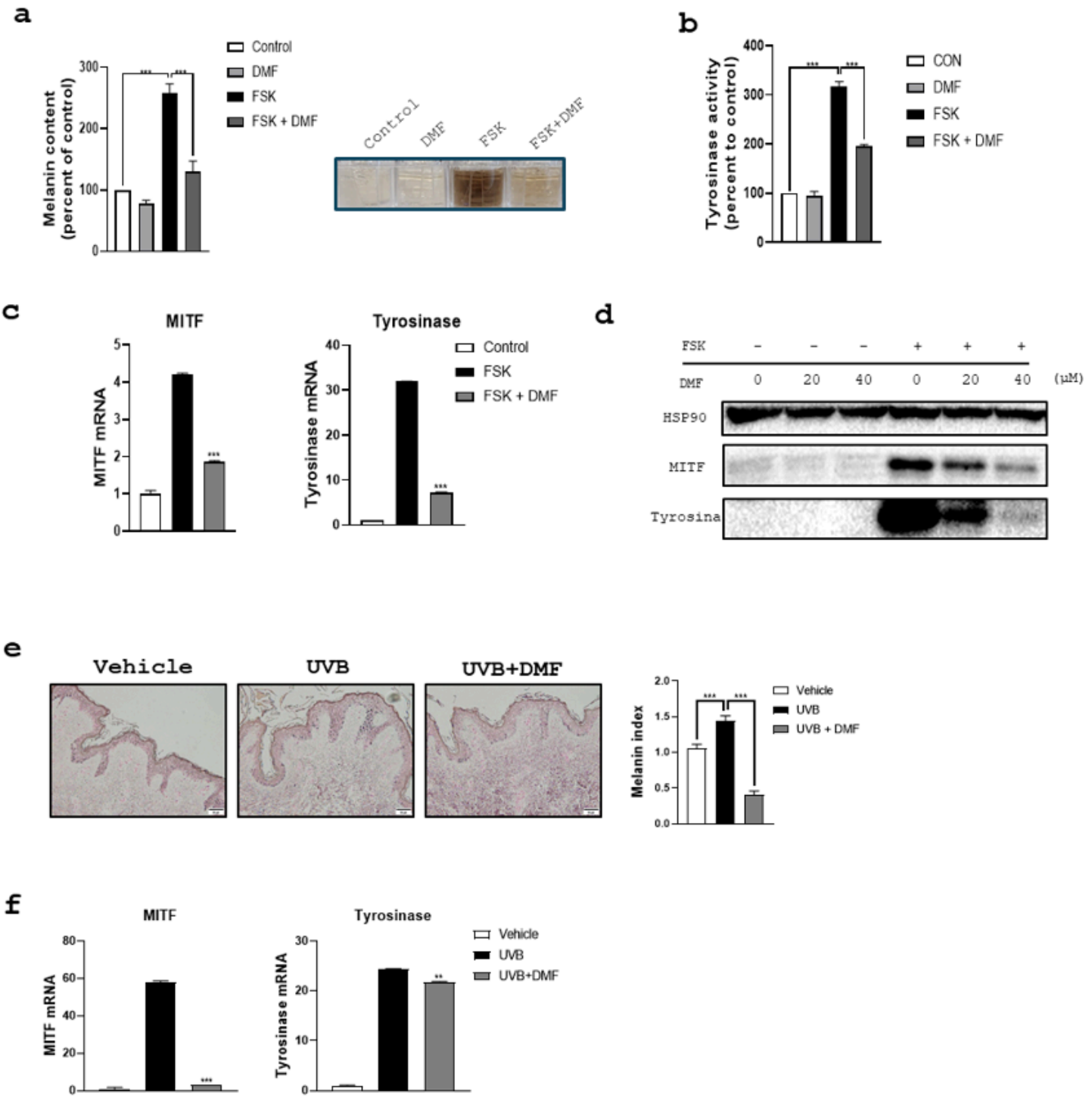


Figure 6

DMF inhibits melanogenesis in melanocytes and ex vivo human skin.

(a) Melanin content (left) and representative images of solubilized melanin (right) in Mel-ab cells stimulated with FSK in the presence or absence of DMF (left) and (b) tyrosinase activity of Mel-ab cells stimulated with FSK in the presence or absence of DMF. (c) qRT-PCR analysis of *Mitf* and *Tyr* mRNA expression in Mel-ab cells. (d) Western blot analysis of Mitf and Tyrosinase protein levels in Mel-ab cells. (e) Representative Fontana-Masson staining images and melanin index quantification in UVB-irradiated

ex vivo human skin treated with or without DMF. (f) Quantitative PCR analysis of *MITF* and *Tyr i*n ex vivo human skin samples.

Supplementary Files

This is a list of supplementary files associated with this preprint. Click to download.

- SupplementaryInformation20260710.docx